7th European Thermal-Sciences Conference (Eurotherm2016) IOP Publishing
Journal of Physics: Conference Series **745** (2016) 032099 doi:10.1088/1742-6596/745/3/032099

Effects of flow maldistribution on the thermal performance of cross-flow micro heat exchangers

C Nonino and S Savino

DPIA, Università degli Studi di Udine, 33100 Udine, Italy

E-mail: carlo.nonino@uniud.it

Abstract. The combined effect of viscosity- and geometry-induced flow maldistribution on the thermal performance of cross-flow micro heat exchangers is investigated with reference to two microchannel cross-sectional geometries, three solid materials, three mass flow rates and three flow nonuniformity models. A FEM procedure, specifically developed for the analysis of the heat transfer between incompressible fluids in cross-flow micro heat exchangers, is used for the numerical simulations. The computed results indicate that flow maldistribution has limited effects on microchannel bulk temperatures, at least for the considered range of operating conditions.

1. Introduction

In heat exchanger design, calculations are usually based on the assumption of uniform velocity distributions in the flow passages even if this hypothesis is not realistic under actual operating conditions. On the other hand, the detrimental effects of flow maldistribution on the performance of macro-scale heat transfer devices are well known [1,2]. Flow maldistribution phenomena can be divided into two classes [3]: (i) geometry-induced maldistribution (mainly due to poor header design) and (ii) viscosity-induced maldistribution (due to temperature dependence of fluid viscosity).

The cross-flow configuration is a flow arrangement often adopted in heat exchanger design. As early as 1978, Chiou [4] analyzed numerically the effects of the two-dimensional flow maldistribution on one fluid side in unmixed-unmixed, cross-flow heat exchangers. Later, Ranganayakulu *et al* used the finite element method to study the effects of flow maldistribution on both fluid sides in plate-and-fin compact heat exchangers, first with constant and variable heat transfer coefficients [5] and then also taking into account the effects of heat conduction in the solid walls [6]. More recently, Zhang [7] studied the flow maldistribution in the same type of heat exchangers by treating the plate-fin core as a porous medium. In all cases the working fluid is assumed to be air. Several articles also deal with the flow maldistribution in micro heat exchangers and micro reactors, dealing, in particular, with the influence of the header geometry [8-12]. Since, however, none of these investigations considers the cross-flow arrangement, there seems to be a lack in the knowledge-base on the effects of nonuniformities in the flow distribution in cross-flow micro heat exchangers, which, for several aspects, are different from heat exchangers of large size having the same flow configuration.

The present authors have recently developed a FEM procedure for the analysis of the heat transfer between incompressible fluids (liquids) in cross-flow micro heat exchangers [13]. An improved version has been used to study the effects of the viscosity-induced flow maldistribution, i.e., the lack of uniformity in microchannel average velocity stemming from the temperature dependence of fluid viscosity [14]. In this paper, the same procedure is employed to investigate the combined effect of

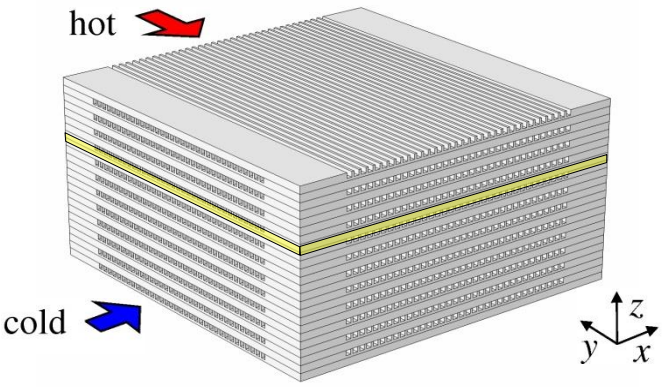

Figure 1. Structure of the core of a cross-flow micro heat exchangers. Yellow: computational domain.

viscosity- and geometry-induced flow maldistribution on the thermal performance of cross-flow micro heat exchangers with reference to two microchannel cross-sectional geometries, three solid materials and three mass flow rates. Three velocity nonuniformity models are considered.

2. Physical model

The effects of flow maldistribution in cross-flow micro heat exchangers are studied using a finite element procedure specifically developed for the analysis of fluid flow and heat transfer in micro heat exchangers of that type [13,14]. The active part (core) of a cross-flow micro heat exchanger consists of several layers of microchannels arranged in such a way that the flow direction in each layer is perpendicular to that of the adjacent layers, as illustrated in figure 1. With reference to the portion of the core away from the external surfaces parallel to the microchannel layers, it is possible to exploit the existing symmetries to study the thermal performance of a cross-flow micro heat exchanger by solving numerically the energy equation in a domain corresponding to a repetitive portion of the core that includes two half-layers of microchannels (one for the cold and one for the hot fluid) and the solid wall in between (shown in yellow in figure 1).

The analysis is carried out on the basis of the following assumptions:

- all microchannels are equal;
- the hot fluid and the cold fluid are the same liquid and have the same mass flow rate;
- on each external side, convective heat transfer takes place with a fluid at a temperature equal to the weighted average of the appropriate inlet or outlet microchannel bulk temperatures;
- flow maldistribution is one-dimensional since only one slice of the core is analyzed;
- viscosity and thermal conductivity of the fluid are constant within each microchannel, but they can be different in different microchannels, with values based on microchannel average temperatures to allow accounting for viscosity-induced flow maldistribution;
- the effects of geometry-induced flow maldistribution can be determined from suitable loss coefficients to be used in the calculation of microchannel pressure drops.

Obviously, following this approach it is only possible to consider the uneven flow distribution among microchannels of the same layer. The analysis of the flow maldistribution among different layers of microchannels would require a detailed simulation of the flow and heat transfer in the entire micro heat exchanger and, consequently, the availability of massive computational resources.

3. Governing equations

The steady-state incompressible flow in each microchannel is governed by the Navier-Stokes equations which can be solved in their parabolised form, provided that the Reynolds number is larger than about 50 so that diffusion of momentum in the axial direction can be neglected [15]

$$\frac{\partial U}{\partial X}+\frac{\partial V}{\partial Y}+\frac{\partial W}{\partial Z}=0 \qquad (1)$$

$$\rho_f U \frac{\partial U}{\partial X} = \mu \left(\frac{\partial^2 U}{\partial Y^2} + \frac{\partial^2 U}{\partial Z^2} \right) - \rho_f \left(V \frac{\partial U}{\partial Y} + W \frac{\partial U}{\partial Z} \right) - \frac{d\overline{P}}{dX} \tag{2}$$

$$\rho_f U \frac{\partial V}{\partial X} = \mu \left(\frac{\partial^2 V}{\partial Y^2} + \frac{\partial^2 V}{\partial Z^2} \right) - \rho_f \left(V \frac{\partial V}{\partial Y} + W \frac{\partial V}{\partial Z} \right) - \frac{\partial P}{\partial Y} \tag{3}$$

$$\rho_f U \frac{\partial W}{\partial X} = \mu \left(\frac{\partial^2 W}{\partial Y^2} + \frac{\partial^2 W}{\partial Z^2} \right) - \rho_f \left(V \frac{\partial W}{\partial Y} + W \frac{\partial W}{\partial Z} \right) - \frac{\partial P}{\partial Z} \tag{4}$$

In the above equations, X, Y and Z are the axial and the transverse Cartesian coordinates in the single microchannel reference system, U, V and W are the axial and the transverse velocity components, P is the deviation from the hydrostatic pressure and $\overline{P}$ is its average value over the cross-section, while μ represents the dynamic viscosity of the fluid. On rigid boundaries, the no-slip conditions, that is, $U = V = W = 0$, are imposed. Finally, the step-by-step solution of Eqs. (1) to (4) requires an inlet condition which here is assumed as $U = U_{in}$ and $V = W = 0$, being U_{in} a uniform inlet velocity.

The heat transfer in the considered computational domain is governed by the energy equation in its elliptic form

$$\rho c \left(u \frac{\partial t}{\partial x} + v \frac{\partial t}{\partial y} + w \frac{\partial t}{\partial z} \right) = \frac{\partial}{\partial x} \left(k \frac{\partial t}{\partial x} \right) + \frac{\partial}{\partial y} \left(k \frac{\partial t}{\partial y} \right) + \frac{\partial}{\partial z} \left(k \frac{\partial t}{\partial z} \right) \tag{5}$$

where x, y and z are the global Cartesian coordinates in the heat exchanger reference system and u, v and w are the corresponding velocity components. The symbol t indicates temperature, while ρ, c and k represent density, specific heat and thermal conductivity, which are equal to ρ_f, c_f and k_f in the fluid and to ρ_s, c_s and k_s in the solid. Obviously, in the parts of the computational domain corresponding to solid walls we have $u = v = w = 0$. Dirichlet conditions $t = t_{c,i}$ and $t = t_{h,i}$ are specified on the portions of the boundaries coinciding with the microchannel inlets, being $t_{c,i}$ and $t_{h,i}$ the entrance temperature of the cold and hot fluids, respectively. Instead, the standard Neumann conditions $\partial t/\partial n = 0$ are imposed on outflow boundaries. The boundary conditions on the external solid boundaries where convective heat transfer with the surrounding fluid takes place are $-k\,\partial t/\partial n = \alpha\,(t - t_a)$, where n is the outward normal to the boundary, α is the convection coefficient and t_a is the temperature of the surrounding fluid. Finally, symmetry conditions on planes perpendicular to the z-axis are $\partial t/\partial z = 0$.

4. Solution procedure

The numerical simulations have been carried out using a finite element procedure specifically developed for the analysis of the heat transfer between incompressible fluids in cross-flow micro heat exchangers. A detailed description is reported in [13,14], while only the main features are summarized below:

- an in-house FEM code for the solution of Eqs. (1) to (4) is used first to compute the velocity field and the pressure drop in a single microchannel;
- then, an appropriate mapping of the velocity field (U,V,W) thus determined is used to obtain the velocity components (u,v,w) in the fluid parts of the three-dimensional computational domain where the energy equation (5) is solved using another in-house FEM code;
- a domain decomposition technique is adopted to allow a separate meshing of the parts of the domain corresponding to each half-layer of microchannels plus one half of the solid wall in between, using grids with optimal nodal densities but not matching at the common interface;
- pressure drop in headers is accounted for by means of suitable loss coefficients ξ_j, which can be different for different microchannels (subscript j refers to the generic microchannel);
- nonuniform distributions of microchannel average velocities u_j are computed through an iterative technique on the basis of two constraints: (i) the total mass flow rate must have the desired value and (ii) the total pressure drop $\Delta p_{j,TOT}$, sum of the contributions $\Delta p_{j,micr}$ from the microchannel and $\Delta p_{j,head}$ from the header,

$$\Delta p_{j,TOT} = \Delta p_{j,micr} + \Delta p_{j,head} = \Delta p_{j,micr} + \xi_j \, \rho_f \, \frac{u_j^2}{2}$$

must be the same in all microchannels of each layer even if pressure loss coefficients or average fluid viscosities are different. Entrance effects are accounted for in the calculation of $\Delta p_{j,micr}$.

The procedure has been validated in [13,14] through comparisons of results of numerical simulations with experimental data obtained by Brandner *et al* [16] for a cross-flow micro heat exchanger consisting of 50 stainless steel foils with 34 rectangular microchannels per foil.

5. Results and discussion

The effects of geometry-induced flow maldistribution are analyzed with reference to two of the micro heat exchanger geometries, three of the mass flow rates and the three materials considered in [14]. All microchannels are identical and can have (i) a rectangular cross-section, with a height of 100 μm and a width of 200 μm, or (ii) a square cross-section, with a height and a width of 200 μm. The core of the device results from the assembly of foils with 34 microchannels each. The number of foils is 50 (25 fluid layers and 850 microchannels per pass) in the case of the rectangular microchannel cross-section and, to have nearly the same total cross-sectional area per pass, 24 (12 fluid layers and 408 microchannels per pass) in the case of the square microchannel cross-section. In both cases, the thickness of the wall between microchannels of the same layer and between layers of microchannels is 100 μm. The sides of each foil parallel to the microchannels have 2 mm borders. Therefore, the length of the microchannels is 14 mm and the interface between two adjacent layers has an extension of 14 mm ×14 mm. On the bases of the grid independence tests reported in [14], the computational domain, corresponding to two half-layers of microchannels plus the solid in between, as shown in figure 1, has been discretized using a grid with 9,907,200 eight-node hexahedral elements and 10,768,966 nodes.

As in [14], the materials assumed for the cores are copper (k_s = 400 W/(m K)), stainless steel (k_s = 15 W/(m K)) and glass (k_s = 1 W/(m K)), often used for microreactor fabrication [17], the working fluid is water and the inlet temperatures of the cold and the hot streams are 10°C and 95°C, respectively. The values of the convection coefficients are 60,000 W/(m^2 K) and 44,000 W/(m^2 K) on the inlet sides and 30,000 W/(m^2 K) and 22,000 W/(m^2 K) on the outlet sides for the rectangular and the square microchannel geometries, respectively. The values of density and specific heat of water are assumed constant and equal to 985 k/m^3 and 4190 J/(Kg K), while those for temperature dependent viscosity and thermal conductivity have been estimated using the REFPROP 8.0 package [18]. The mass flow rates $\dot{m}$ of the hot and cold fluids are the same (symmetrical throughput) and are equal to 21, 81 and 150 kg/h. The corresponding mean velocities u_0 in the microchannels of each pass are around 0.35, 1.4 and 2.5 m/s with the three mass flow rates. Three microchannel velocity nonuniformity models are specified by means of suitable loss coefficients ξ_j to be used in the calculation of microchannel pressure drops. These coefficients have been determined on the bases of a preliminary analysis assuming that they are representative of possible flow maldistributions that can be found with the three types of headers schematically represented in the top part of figure 2 and identified as I-type, Z1-type and Z2-type. The values of the corresponding loss coefficients are reported, for each microchannel, in the bottom part of the same figure.

Due to the large number of numerical simulations, not all the results can be reported here, but just some examples. In figure 3 the relative average velocity u_j/u_0 in each microchannel of the hot and cold layers is reported for the three types of headers and the three values of the mass flow rate considered. Reference is made to the stainless steel core and the rectangular microchannel cross-section. In all cases, the microchannel average velocity distributions are compared with those obtained for the same test cases when only the viscosity-induced flow maldistribution (VIFM) is accounted for (solid lines). As can be seen in figure 3, with the adopted values of the loss coefficients and the lowest value of the mass flow rate, the magnitude of the geometry-induced flow maldistribution is comparable to the one induced by viscosity, especially for the hot fluid. Instead, with larger values of the mass flow rate, the effect of variations of fluid viscosity among different microchannel becomes almost irrelevant and the

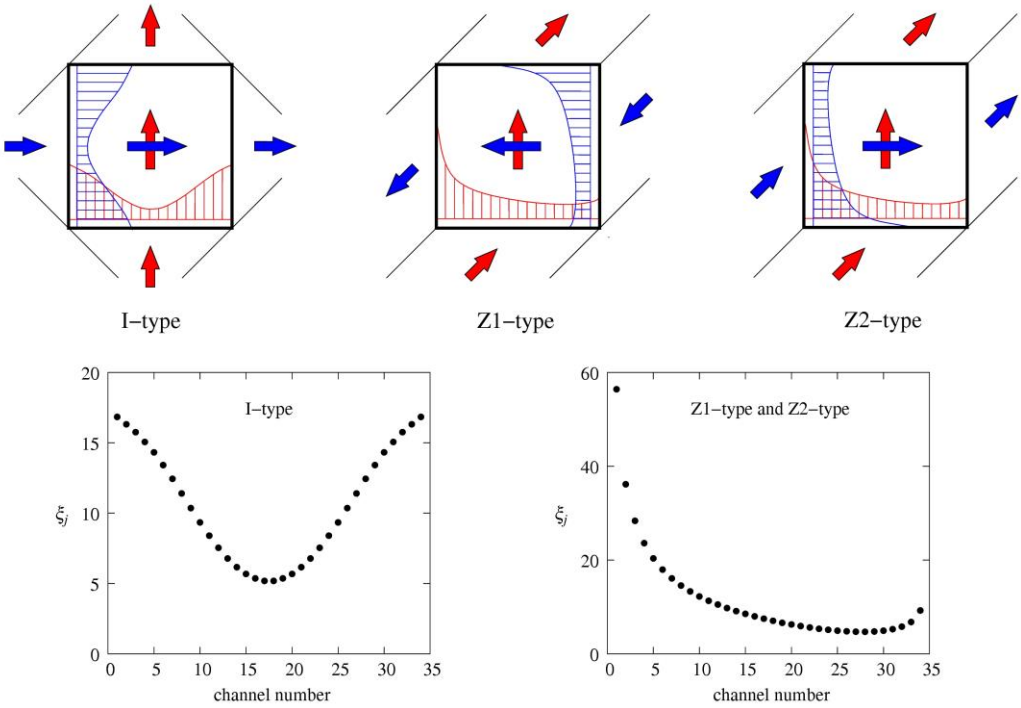

Figure 2. Flow nonuniformity models. Top: types of headers with the corresponding distribution of the pressure loss coefficients; bottom: values of the microchannel pressure loss coefficients.

influence of the header geometry is prevailing. The deviations of the microchannel average velocities u_j with respect to the mean velocity u_0 can be in excess of ±30%. The corresponding relative microchannel outlet bulk temperatures $t_{b,j}/t_{b,0}$, where $t_{b,0}$ is the weighted average of the $t_{b,j}$, are reported in figure 4. It is apparent that, in spite of the significant flow maldistributions shown in figure 3, the nonuniformity of the microchannel outlet bulk temperatures is rather mild, with deviations that never exceed ±10% and, actually, in most of the cases are much lower than that. Since for glass and copper as solid materials the distributions of relative velocities and relative microchannel outlet bulk temperatures show the same trends of those for stainless steel presented in figures 3 and 4, they are not reported here. The microchannel cross-sectional geometry also has a limited impact on the microchannel velocity distributions. In fact, those obtained for the square cross-section are qualitatively similar to those yielded by the rectangular one for the same material, mass flow rate and flow maldistribution model. Therefore, due to the lack of space, also the plots concerning the square cross-section are not shown here. It can be inferred that the effect of material and cross-sectional geometry on the microchannel bulk temperature profiles which, in turn, are related to the viscosity-induced flow maldistribution, is much smaller than that of mass flow rate and header geometry.

The total heat flow rates computed for the same core geometries, materials and mass flow rates considered in this study are reported in [14] in the hypothesis that only viscosity-induced flow maldistribution is present. Here, instead, the heat flow rates influenced by the combined effect of viscosity-induced and geometry-induced flow maldistribution have been computed. To illustrate the effects on heat transfer of the geometry-induced flow maldistribution alone, the maximum percentage variations between the total heat flow rates obtained for the present test cases and the corresponding ones in [14] are reported in table 1 for all the considered combinations of cross-sectional geometries, solid materials and flow nonuniformity models. In all cases, the maximum variations of the heat flow rate are obtained with the largest of the mass flow rates, i.e., $\dot{m} = 150$ kg/h. As can be seen, the variations are always negative, i.e., flow maldistribution causes a reduction of the heat flow rate in the device. However, the magnitude of the reduction is rather small with all the flow maldistribution

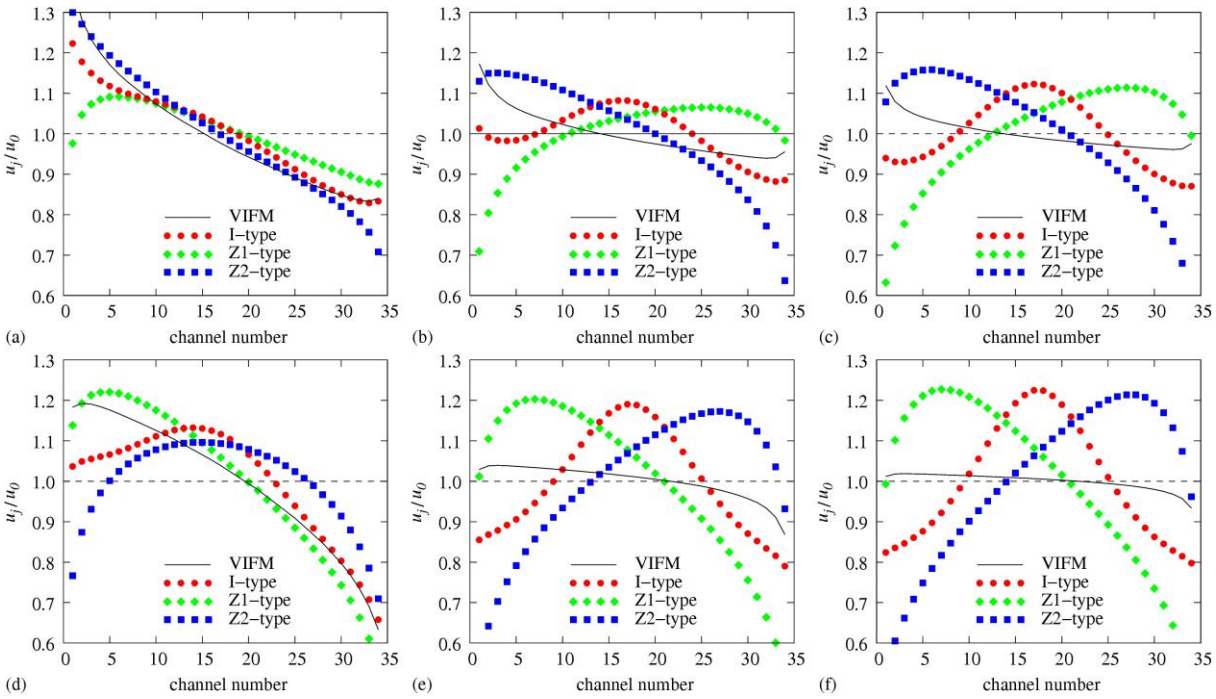

Figure 3. Relative microchannel average velocities u_j/u_0 in stainless steel micro heat exchangers with rectangular microchannel cross-sections. Top: hot fluid; bottom: cold fluid; (a) and (d): $\dot{m} = 21$ kg/h; (b) and (e): $\dot{m} = 81$ kg/h; (c) and (f): $\dot{m} = 150$ kg/h.

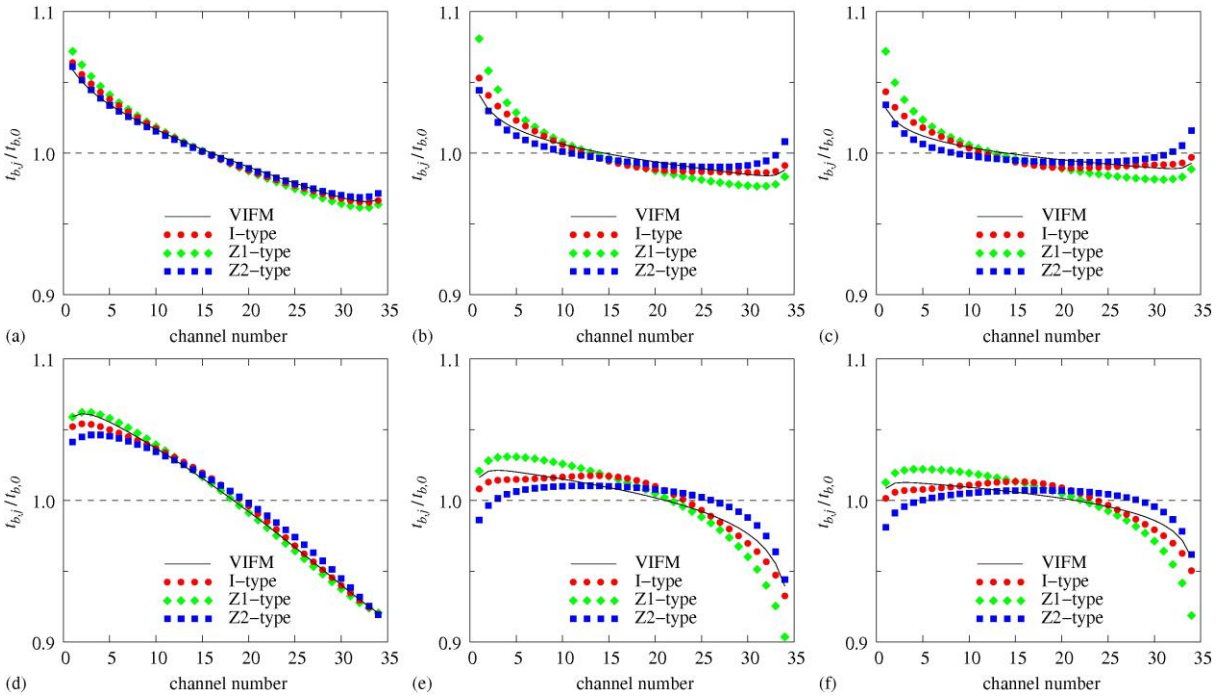

Figure 4. Relative microchannel outlet bulk temperatures $t_{b,j}/t_{b,0}$ in stainless steel micro heat exchangers with rectangular microchannel cross-sections. Top: hot fluid; bottom: cold fluid; (a) and (d): $\dot{m} = 21$ kg/h; (b) and (e): $\dot{m} = 81$ kg/h; (c) and (f): $\dot{m} = 150$ kg/h.

Table 1. Maximum percentage variation of the heat flow rate for different cross-sectional geometries, solid materials and flow maldistribution models.

	rectangular cross-section			square cross-section		
	I-type	Z1-type	Z2-type	I-type	Z1-type	Z2-type
glass	-0.29	-0.69	-0.70	-0.47	-0.92	-0.89
steel	-0.69	-1.25	-1.27	-0.98	-1.74	-1.56
copper	-0.72	-1.05	-1.12	-0.99	-1.38	-1.33

models considered, in spite of the marked nonuniformity of the velocity distributions. In any event, it must be pointed out that even if the thermal performance deterioration appears rather limited, flow maldistribution implies different residence times of the fluid in the microchannels, and this can represent a problem if a device operates as a microreactor [19]. Direct comparisons with the results of Chiou [4] and Ranganayakulu *et al* [5,6] are not possible because in those papers not only the flow maldistribution models, but also the considered ranges of NTU are significantly different since the NTU values for the micro heat exchangers are much smaller than the values typical of the plate-fin heat exchangers considered in the previous investigations.

Finally, to give further insight into the heat transfer process in cross-flow micro heat exchangers, temperature (elevation) and relative specific heat flow rate q''/q_0'' (color map) distributions on the midplane between two layers of microchannels are shown in figure 5 with reference to the rectangular cross-sectional geometry, the minimum and the maximum mass flow rates and glass and copper as solid materials. The symbol q_0'' indicates the mean value of the specific heat flow rate on the midplane. It is worth noting the reversal of the heat flow occurring in some regions as a consequence of the axial heat conduction in the solid, especially when copper is the solid material (blue areas).

6. Conclusions

A FEM procedure specifically developed for the analysis of the heat transfer between incompressible fluids in cross-flow micro heat exchangers has been used to study the combined effect of viscosity- and geometry-induced flow maldistribution on the thermal performance of cross-flow micro heat exchangers. The investigation has been carried out with reference to two microchannel cross-sectional geometries, three solid materials, three mass flow rates and three flow nonuniformity models. The computed results show that, at least for the considered range of operating conditions, flow maldistribution has only limited effects on the thermal performance of these devices.

References

[1] Bhutta M M A, Hayat N, Bashir M H, Khan A R, Ahmad K N and Khan S 2012 *Appl. Therm. Eng.* **32** 1–12.
[2] Singh S K, Mishra M and Jha P K 2014 *Renew. Sust. Energ. Rev.* **40** 583–596.
[3] Shah R K, Sekulić D P 1998 Heat exchangers *Handbook of Heat Transfer* ed W M Rohsenow *et al* (New York: Mc Graw-Hill) chapter 17 p. 17.136.
[4] Chiou J P 1978 *J. Heat Trans.-T. ASME* **100** 580-587.
[5] Ranganayakulu Ch, Seetharamu K N, Sreevastan K V 1997 *Int. J. Heat Mass Tran.* **40** 27–38.
[6] Ranganayakulu Ch and Seetharamu K N 2000 *Heat Mass Transfer* **36** 247–256.
[7] Zhang L Z 2009 *Int. J. Heat Mass Tran.* **52** 4500-4509.
[8] Pan M, Tang Y, Pan L and Lu L 2008 *Chem. Eng. J.* **137** 339–346.
[9] Chein R and Chen J 2009 *Int. J. Therm. Sci.* **48** 1627–1638.
[10] Griffini G and Gavriilidis A 2007 *Chem. Eng. Technol.* **30** 395–406.
[11] Vásquez-Alvarez E, Degasperi F T, Morita L G, Gongora-Rubio M R and Giudici R 2010 *Braz, J. Chem. Eng*. **27** 483–497.
[12] Rebrov E V, Schouten J C, de Croon M H J M 2011 *Chem. Eng. Sci.* **66** 1374–1393.

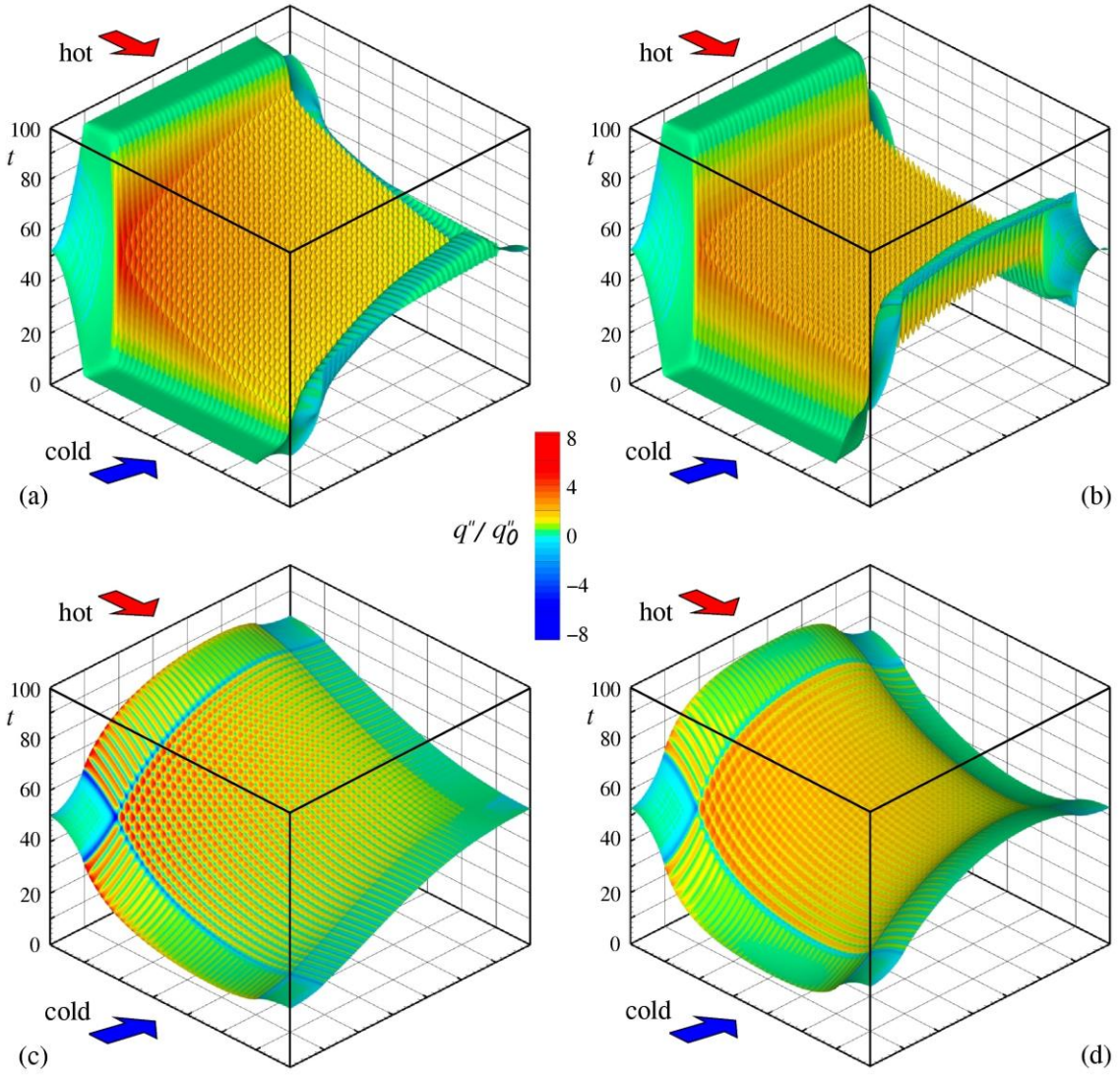

Figure 5. Temperature (elevation) and relative specific heat flow rate q''/q_0'' (color map) distributions on the midplane between two layers of rectangular microchannels. (a): glass, $\dot{m} = 21$ kg/h; (b): glass, $\dot{m} = 150$ kg/h; (c): copper, $\dot{m} = 21$ kg/h; (d): copper, $\dot{m} = 150$ kg/h.

[13] Nonino C, Savino S. and Del Giudice S 2015 *Int. J. Numer. Methods Heat Fluid Flow* **25** 1322–1339.
[14] Nonino C and Savino S 2016 *Int. J. Numer. Methods Heat Fluid Flow* (accepted for publ.).
[15] Shah R K and London A L 1978 *Laminar Flow Forced Convection in Ducts* (New York: Academic Press).
[16] Brandner J J, Henning T, Schygulla U, Wenka A, Zimmermann S and Schubert K *2005 Proc. ICMM2005 (Toronto)* paper No. ICMM2005–75072 (on CD-ROM).
[17] Hessel V, Schouten J C, Renken A and Yoshida J-I 2009 *Handbook of Micro Reactors* (Weinheim; Wiley-VCH).
[18] Lemmon EW, Huber, M L, McLinden M O 2007 *REFPROP, Version 8.0*, (Gaithersburg: National Institute of Standards and Technology).
[19] Schubert K, Brandner J, Fichtner M, Linder G, Schygulla U and Wenka A 2001 *Microscale Therm. Eng.* **5** 17–39.